# Up-regulation of Cav$\beta_3$ Subunit in Primary Sensory Neurons Increases Voltage-activated Ca$^{2+}$ Channel Activity and Nociceptive Input in Neuropathic Pain*

**Li Li (李莉)**[‡§]**, Xue-Hong Cao (曹雪红)**[‡§]**, Shao-Rui Chen (陈少瑞)**[‡§]**, Hee-Dong Han (한희동)**[¶‖]**, Gabriel Lopez-Berestein**[¶‖]**, Anil K. Sood**[‖]**, and Hui-Lin Pan (潘惠麟)**[‡§‖]1

*From the* ‡*Center for Neuroscience and Pain Research, Departments of* §*Anesthesiology and Perioperative Medicine and* ¶*Experimental Therapeutics, and* ‖*Center for RNA Interference and Non-Coding RNA, University of Texas M.D. Anderson Cancer Center, Houston, Texas 77030*

**Background:** We determined how nerve injury affects calcium channel $\beta$ (Cav$\beta$) subunits in neuropathic pain.
**Results:** Nerve injury increases Cav$\beta_3$ expression level, and Cav$\beta_3$ knockdown reduces increased calcium channel activity in primary sensory neurons and pain hypersensitivity.
**Conclusion:** Cav$\beta_3$ subunit up-regulation augments calcium channel activity in neuropathic pain.
**Significance:** Understanding molecular changes in sensory neurons is important for developing new treatments for neuropathic pain.

High voltage-activated calcium channels (HVACCs) are essential for synaptic and nociceptive transmission. Although blocking HVACCs can effectively reduce pain, this treatment strategy is associated with intolerable adverse effects. Neuronal HVACCs are typically composed of $\alpha_1$, $\beta$ (Cav$\beta$), and $\alpha_2\delta$ subunits. The Cav$\beta$ subunit plays a crucial role in the membrane expression and gating properties of the pore-forming $\alpha_1$ subunit. However, little is known about how nerve injury affects the expression and function of Cav$\beta$ subunits in primary sensory neurons. In this study, we found that Cav$\beta_3$ and Cav$\beta_4$ are the most prominent subtypes expressed in the rat dorsal root ganglion (DRG) and dorsal spinal cord. Spinal nerve ligation (SNL) in rats significantly increased mRNA and protein levels of the Cav$\beta_3$, but not Cav$\beta_4$, subunit in the DRG. SNL also significantly increased HVACC currents in small DRG neurons and monosynaptic excitatory postsynaptic currents of spinal dorsal horn neurons evoked from the dorsal root. Intrathecal injection of Cav$\beta_3$-specific siRNA significantly reduced HVACC currents in small DRG neurons and the amplitude of monosynaptic excitatory postsynaptic currents of dorsal horn neurons in SNL rats. Furthermore, intrathecal treatment with Cav$\beta_3$-specific siRNA normalized mechanical hyperalgesia and tactile allodynia caused by SNL but had no significant effect on the normal nociceptive threshold. Our findings provide novel evidence that increased expression of the Cav$\beta_3$ subunit augments HVACC activity in primary sensory neurons and nociceptive input to dorsal horn neurons in neuropathic pain. Targeting the Cav$\beta_3$ subunit at the spinal level represents an effective strategy for treating neuropathic pain.

Chronic pain, such as neuropathic pain induced by peripheral nerve injury, leads to prolonged excruciating suffering and a reduced quality of life. However, effective treatment of chronic pain remains a major challenge, with only half of patients receiving adequate pain relief (1). Pain can occur spontaneously or as a result of exposure to mildly painful stimuli (hyperalgesia) or stimuli not normally perceived as painful (allodynia). Our understanding of the mechanisms that sustain chronic neuropathic pain conditions is incomplete. It is likely that neuropathic pain becomes chronic as a result of the plasticity of both peripheral nerves and spinal dorsal horn neurons. Clinical studies of patients with neuropathic pain have indicated that the altered central processing associated with pain is maintained dynamically by ongoing peripheral input (2, 3). However, the molecular mechanisms underlying persistent nociceptive input from primary afferent nerves in neuropathic pain are not fully known.

High voltage-activated calcium channels (HVACCs)[2] are essential for many physiological functions, such as neurotransmitter release, membrane excitability, gene transcription, and synaptic plasticity (4, 5). HVACCs in neurons are typically composed of a pore-forming $\alpha_1$ subunit (the principal component of HVACCs) and accessory $\beta$ (Cav$\beta$), $\alpha_2\delta$, and possibly $\gamma$ subunits (5, 6). HVACCs are clarified as the L (Ca$_v$1.1–1.4)-type, N (Ca$_v$2.2)-type, P/Q (Ca$_v$2.1)-type, and R (Ca$_v$2.3)-type according to the different biophysical and pharmacological properties of their $\alpha_1$ subunits (5, 7). The $\alpha_2\delta$ subunit can augment functional expression of the $\alpha_1$ subunit (8) and is up-regulated in the dorsal root ganglion (DRG) after nerve injury (9). Another important auxiliary subunit, the Cav$\beta$ subunit, is involved in promoting the surface expression of the $\alpha_1$ subunit and the gating properties of HVACCs (10–12). There are four Cav$\beta$ subunits, each with splice variants, encoded by four distinct

1 To whom correspondence should be addressed: Dept. of Anesthesiology and Perioperative Medicine, Unit 110, University of Texas MD Anderson Cancer Center, 1515 Holcombe Blvd., Houston, TX 77030. Tel.: 713-563-0822; Fax: 713-794-4590; E-mail: huilinpan@mdanderson.org.

2 The abbreviations used are: HVACC, high voltage-activated calcium channels; DRG, dorsal root ganglion; EPSC, excitatory postsynaptic current; SNL, spinal nerve ligation.

genes. The Cav$\beta_1$ subunit appears to be the only Cav$\beta$ subunit expressed in the skeletal muscle (13), whereas the Cav$\beta_2$ subunit is present primarily in the heart (14). The Cav$\beta_3$ subunit is strongly expressed in smooth muscle and brain, and the Cav$\beta_4$ is the predominant subunit in cerebellum (14, 15). Mice deficient in Cav$\beta_1$ or Cav$\beta_2$ are not viable (16, 17), and knock-out of Cav$\beta_3$ or Cav$\beta_4$ results in a wide range of abnormalities (18, 19). Despite the importance of Cav$\beta$ subunits in regulating HVACC activity, little is known about the contribution of Cav$\beta$ subunits to nerve injury-induced changes in HVACC activity in primary sensory neurons and neuropathic pain.

Therefore, we used a rat model of neuropathic pain to determine how nerve injury affects the expression level of Cav$\beta$ subunits in the DRG and dorsal spinal cord. We also determined the contribution of the Cav$\beta_3$ subunit to increased HVACC activity in DRG neurons and nociceptive input to the spinal cord induced by nerve injury. Our findings indicate that among the four Cav$\beta$ subunits in the DRG and spinal cord, Cav$\beta_3$ and Cav$\beta_4$ showed the greatest expression. Nerve injury up-regulated the Cav$\beta_3$, but not Cav$\beta_4$, subunit in the DRG. Furthermore, siRNA knockdown of Cav$\beta_3$ greatly reduced increased HVACC activity in the DRG, glutamatergic input to the spinal cord, and pain hypersensitivity caused by nerve injury without impairing normal nociception. Our study highlights the important role of the Cav$\beta_3$ subunit in increased HVACC activity in primary sensory neurons in neuropathic pain. Therefore, targeting the Cav$\beta_3$ subunit at the spinal level represents a new strategy for treating neuropathic pain with improved therapeutic profiles.

## EXPERIMENTAL PROCEDURES

*Neuropathic Pain Model and Intrathecal Cannulation*—Neuropathic pain was induced by SNL in rats, as described previously (20, 21). In brief, male Sprague-Dawley rats initially weighing ~250 g (Harlan, Indianapolis, IN) were anesthetized with use of 2% isoflurane. The left L5 and L6 spinal nerves were isolated under a surgical microscope and ligated with 4.0 silk suture. Sham surgery was performed in the contralateral side of the same rats or separate rats by using the same procedure except that the spinal nerves were not ligated. In some rats, intrathecal cannulation was performed 7 days after SNL. After rats were anesthetized with isoflurane, catheters (PE-10 polyethylene tubing, 8 cm) were inserted through an incision in the cisternal membrane and advanced caudally so that the tip of each catheter was positioned at the lumbar spinal level (22, 23). The catheters were externalized to the back of the neck and sutured to the musculature and skin at the incision site. All experiments were approved by the Animal Care and Use Committee of the University of Texas MD Anderson Cancer Center and conformed to National Institutes of Health guidelines on the ethical use of animals.

*Nociceptive Behavioral Tests*—To assess mechanical nociception, paw withdrawal thresholds were measured by applying a noxious pressure stimulus using an Ugo Basil Analgesimeter (Varese, Italy). The nociceptive threshold was recorded when rats displayed pain by paw withdrawal or vocalization. The cutoff of 400 g was used to avoid potential tissue injury (22).

The tactile withdrawal threshold was measured by application of von Frey filaments to both hind paws of SNL rats. Rats were placed individually in plastic cages on a mesh floor and then allowed to acclimate for at least 30 min. A series of calibrated von Frey filaments (Stoelting Co., Wood Dale, IL) were applied perpendicularly to the plantar surface of the hind paw. Brisk withdrawal or paw flinching was considered a positive response. The tactile stimulus that could produce a 50% likelihood of withdrawal was determined by using the "up-down" calculating method (21, 24).

*Isolation of DRG Neurons and Electrophysiological Recording of HVACCs*—Dissociation of DRG neurons was performed essentially as we described previously (25, 26). Rats were anesthetized with isoflurane and then rapidly decapitated. The lumbar segment of the vertebral column was removed quickly. The L5 and L6 DRGs were obtained and transferred into cold DMEM (Invitrogen). After DRGs were minced, they were placed into 5 ml of DMEM containing trypsin (type I, 0.2 mg/ml; Sigma) and collagenase (type I, 1 mg/ml; Sigma). After incubation at 34 °C for 40 min, 10% FBS was used to stop trypsin digestion. Neurons were plated onto a 35-mm culture dish containing poly-L-lysine (50 μg/ml) precoated coverslips. The cells were incubated in fresh medium for at least another hour before they were used for electrophysiological recording of HVACC activity.

HVACC currents were measured using barium as the charge carrier ($I_{Ba}$) (25, 26). Electrodes with a resistance of 2–3 megohms were pulled from glass capillaries and fire-polished. After establishing the whole-cell configuration, the cell membrane capacitance and series resistance were electronically compensated. Signals were processed with use of an EPC-10 amplifier (HEKA Instruments, Lambrecht, Germany), filtered at 1 kHz, digitized at 10 kHz, and acquired by using the Pulse program (HEKA Instruments). The extracellular solution consisted of 140 mM tetraethylammonium, 2 mM $MgCl_2$, 3 mM $BaCl_2$, 10 mM glucose, and 10 mM HEPES (pH 7.4, osmolarity of 320 mosM). The pipette internal solution consisted of 120 mM CsCl, 1 mM $MgCl_2$, 10 mM HEPES, 10 mM EGTA, 4 mM MgATP, and 0.3 mM NaGTP (pH 7.2, osmolarity of 300 mosM). The voltage-dependent activation of HVACCs was tested at a holding potential of −90 mV and elicited by a series of command potentials from −70 to 50 mV for 150 ms in 10-mV steps (5-s intervals). The voltage-dependent inactivation of HVACCs was assessed by depolarizing cells to a series of prepulse potentials from −90 to 10 mV for 500 ms, followed by a command potential to 0 for 150 ms (25, 26). All experiments were performed at room temperature (~25 °C).

*Spinal Cord Slice Preparation and Electrophysiological Recording of Synaptic Activity*—After rats were anesthetized with 2–3% isoflurane, the lumbar segment of the spinal cord at the L5/L6 level was removed through laminectomy. The spinal cord tissue was immediately placed in ice-cold sucrose artificial cerebrospinal fluid presaturated with 95% $O_2$ and 5% $CO_2$. The sucrose artificial cerebrospinal fluid contained 234 mM sucrose, 3.6 mM KCl, 1.2 mM $MgCl_2$, 2.5 mM $CaCl_2$, 1.2 mM $NaH_2PO_4$, 12 mM glucose, and 25 mM $NaHCO_3$. The tissue was then placed in a shallow groove formed in a gelatin block and glued onto the stage of a vibratome. Transverse spinal cord slices (400 μm)

**TABLE 1**
List of primers used in PCR-agarose gel analysis

| Gene (accession no.) | Primers |
|---|---|
| Ca$_V$β$_1$ (NM_017346.1) | Fwd: 5′-CACACCCGCCTAGCAGGACG-3′<br>Rev: 5′-CGGCCCCGGTTCCTGTTGTC-3′ |
| Ca$_V$β$_2$ (NM_053851.1) | Fwd: 5′-AGTGGTGTTGGTGGGCCCCT-3′<br>Rev: 5′-ACTCCTGCGGGGGACACTGG-3′ |
| Ca$_V$β$_3$ (NM_012828.2) | Fwd: 5′-AACCACCCAGCACAGCTAGCC-3′<br>Rev: 5′-CACTGGGCGGACCCAGCATC-3′ |
| Ca$_V$β$_4$ (NM_012828.2) | Fwd: 5′-CACCAGATCCAGCCTAGCGGAA-3′<br>Rev: 5′-TTGTGTGGGTGGCACGCCAAT-3′ |
| GAPDH (NM_012828.2) | Fwd: 5′-TGCCACTCAGAAGACTGTGG-3′<br>Rev: 5′-TTCAGCTCTGGGATGACCTT-3′ |

**TABLE 2**
List of primers used in quantitative PCR
Fwd means forward; Rev means reverse.

| Gene (accession no.) | Primers |
|---|---|
| Ca$_V$β$_1$ (NM_017346.1) | Fwd: 5′-GCGAGCACCTGGCGGAGTAC-3′<br>Rev: 5′-GCGGTAGCCATGGTGCGGTT-3′ |
| Ca$_V$β$_2$ (NM_053851.1) | Fwd: 5′-AGTGGGACAGGTCGAGGCCT-3′<br>Rev: 5′-CACGGTGTGGAACATAGCGGTC-3′ |
| Ca$_V$β$_3$ (NM_012828.2) | Fwd: 5′- TTCACCCCTGGAGCGGGACA-3′<br>Rev: 5′-ACGGTGAGGCTGGTACAGGTC-3′ |
| Ca$_V$β$_4$ (NM_012828.2) | Fwd: 5′-ACCTGGAGGCATATTGGCGTGC-3′<br>Rev: 5′-TGGTTGCTATGCCTCATCCGCT-3′ |
| GAPDH (NM_012828.2) | Fwd: 5′-TGCCACTCAGAAGACTGTGG-3′<br>Rev: 5′-TTCAGCTCTGGGATGACCTT-3′ |

were cut in the ice-cold sucrose artificial cerebrospinal fluid and preincubated in Krebs' solution oxygenated with 95% $O_2$ and 5% $CO_2$ at 34 °C for at least 1 h before they were transferred to the recording chamber. The Krebs' solution contained 117 mM NaCl, 3.6 mM KCl, 1.2 mM MgCl$_2$, 2.5 mM CaCl$_2$, 1.2 mM NaH$_2$PO$_4$, 11 mM glucose, and 25 mM NaHCO$_3$ gassed with 95% $O_2$ and 5% $CO_2$.

Each spinal cord slice was placed in a glass-bottomed chamber and continuously perfused with Krebs' solution at 5.0 ml/min at 34 °C maintained by an in-line solution heater and a temperature controller. The neurons in lamina II (substantia gelatinosa) at the L5 and L6 levels were identified under a fixed-stage microscope (BX50WI; Olympus, Tokyo, Japan) with differential interference contrast/infrared illumination. Lamina II neurons were selected for recording because they primarily receive nociceptive input from peripheral nerve fibers (27, 28). Recordings of excitatory postsynaptic currents (EPSCs) were performed by using the whole-cell voltage clamp method, as we described previously (23, 29, 30). The impedance of the electrode was 5–10 megohms when filled with internal solution containing 135 mM potassium gluconate, 5 mM KCl, 2 mM MgCl$_2$, 0.5 mM CaCl$_2$, 5 mM HEPES, 5 mM EGTA, 5 mM ATP-Mg, 0.5 mM sodium GTP, and 10 mM lidocaine *N*-ethyl bromide (QX314) adjusted to pH 7.2–7.4 with 1 M KOH (290–300 mosM). EPSCs of lamina II neurons were recorded at a holding potential of −60 mV and evoked by electrical stimulation (0.8 mA, 0.2 ms, 0.2 Hz) of the dorsal root (31). At the stimulation intensity used, both A- and C-fiber afferents that were in close contact with the electrode tip were stimulated (30, 32). Signals were processed by an amplifier (MultiClamp 700B; Molecular Devices, Sunnyvale, CA), filtered at 1–2 kHz, digitized at 10 kHz, and stored into a computer with pCLAMP 9.2 (Molecular Devices).

*PCR Analysis*—We used agarose gel electrophoresis to determine which Cavβ subunits are expressed in the DRG and dorsal spinal cord. Because Cavβ subunits have a high "G-C" content, a "slow-down" PCR method was used for PCR amplification as reported previously (33). PCR products were generated with LA Taq$^{TM}$ DNA polymerase (Takara), amplified with use of Cavβ subunit-specific primers, and analyzed with use of agarose gels. The sequence primers of the four Cavβ subunits that were used are shown in Table 1.

We also used real-time PCR to determine the relative mRNA level of the Cavβ subunits. In brief, total RNA was extracted by using an RNeasy mini kit (Qiagen). Reverse transcription was performed with use of SuperScript II (Invitrogen). After treatment with RNase H, the resultant cDNA was quantified by

using an IQ5 system (Bio-Rad). The sequence primers of the Cavβ subunits were listed in Table 2. The mRNA level of the Cavβ subunits was calculated by using the $2^{-\Delta\Delta Ct}$ method and normalized by GAPDH (used as an internal control). The mean values of DRGs and spinal cord tissues contralateral to SNL were considered as 1.

*Western Blot Analysis*—Tissues were sonicated in RIPA buffer and a mixture of protease inhibitors (Sigma). Total protein was extracted by centrifuge at $16,000 \times g$ for 10 min at 4 °C. Equal amounts of proteins (20 μg) were subjected to SDS-PAGE and transferred onto polyvinylidene difluoride membrane (Immobilon P, Millipore). The blot was probed with anti-Cavβ$_2$ (NeuroMab, Davis, CA; 1:1000 dilution), anti-Cavβ$_3$ antibody (Santa Cruz Biotechnology; 1:1000 dilution), anti-Cavβ$_4$ (NeuroMab; 1:1000 dilution), and anti-GAPDH (Millipore; 1:1000 dilution). ImageJ was used to quantify the band intensities. The amounts of Cavβ subunit proteins were normalized by GAPDH, and the mean values of the DRG or spinal cord tissues in the contralateral side of nerve injury were considered as 1.

*Double Immunofluorescence Labeling of Cavβ$_3$ Subunit and NF200 or Peripherin in the DRG*—To determine the cellular distribution of the Cavβ$_3$ subunit in the DRG, we performed double immunofluorescence labeling of this Cavβ$_3$ subunit with a marker for small neurons (peripherin) (34) or a marker for medium and large neurons (NF200) (35). The DRGs from sham and SNL rats were cut to 30 μm and collected free floating in 0.1 M PBS. Sections were rinsed in Tris-HCl buffer and incubated with 1% $H_2O_2$ in TBS for 30 min to quench the endogenous peroxidase. Sections were blocked with 5% blocking reagent (PerkinElmer Life Sciences) in 0.1 M Tris-HCl for 1 h at 25 °C. Then the sections were incubated with the primary antibody mixture as follows: rabbit anti-Cavβ$_3$ (Alomone Labs, Jerusalem, Israel; dilution 1:100) and mouse anti-NF200 (Sigma; dilution 1:200) or mouse anti-peripherin (Abcam, Cambridge, MA; dilution 1:100) at 25 °C for 2 h and at 4 °C overnight. Subsequently, sections were rinsed and incubated with the secondary antibody mixture as follows: peroxidase-conjugated donkey anti-rabbit IgG (Jackson ImmunoResearch; dilution 1:100) and Alexa Fluor-594-conjugated donkey anti-mouse IgG (Molecular Probes, Eugene, OR; dilution 1:400) for 2 h at room temperature. Then the sections were rinsed and incubated with fluorescein tyramide (PerkinElmer Life Sciences; dilution 1:100) for 10 min. Finally, the sections were rinsed, mounted on slides, dried, and coverslipped. The negative control was established by omitting the primary antibody.
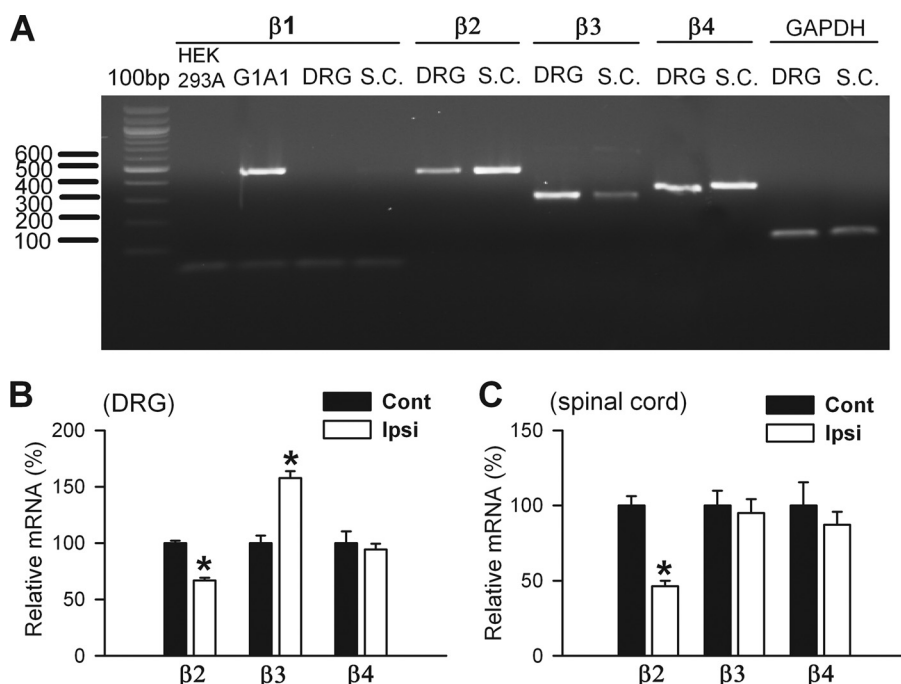
FIGURE 1. **Effect of nerve injury on the mRNA level of Cavβ subunits in the DRG and dorsal spinal cord tissues.** *A,* agarose gel electrophoresis showing the presence of the DNA products of Cavβ$_2$, Cavβ$_3$, and Cavβ$_4$ subunits in the DRG and dorsal spinal cord (*S.C.*) tissues from control rats. G1A1 cells stably expressing Cavβ$_1$ were used as a positive control for the Cavβ$_1$ subunit, and the HEK293A cell line was used as a negative control. *B,* group data show the effect of SNL on the mRNA level of Cavβ$_2$, Cavβ$_3$, and Cavβ$_4$ subunits in the DRG (*n* = 4 in each group). *C,* summary data show the effect of SNL on the mRNA level of Cavβ$_2$, Cavβ$_3$, and Cavβ$_4$ subunits in the dorsal spinal cord (*SC*) (*n* = 4 in each group). *Ipsi,* ipsilateral (nerve injury) side; *Cont,* contralateral (control) side. *, $p < 0.05$, compared with the corresponding value on the contralateral (control) side.

The sections were examined on a laser-scanning confocal microscope (Carl Zeiss, Jena, Germany), and the areas of interest were photo-documented. To quantify changes in the distribution of Cavβ$_3$ in peripherin- and NF200-immunoreactive DRG neurons by nerve injury, four confocal images were randomly selected from each DRG (two DRGs/rat) in three control and three nerve-injured rats, and the total number of peripherin- and NF200-immunoreactive cell bodies with and without Cavβ$_3$ labeling was counted from each section.

*Chitosan-siRNA Preparation and Intrathecal Injection*—All of the siRNA was purchased from Integrated DNA Technologies (San Diego). Two Cavβ$_3$-specific siRNAs (IDT catalog numbers 57372397 and 57372400) and a control siRNA (IDT catalog number 58008661; target sense, CGUUAAUCGCGU-AUAAUACGCGUAT) were diluted by using RNA-free duplex buffer (1 µg/µl), incubated at 94 °C for 2 min for annealing, and then cooled slowly to room temperature (~25 °C). We used chitosan to conjugate the siRNA for intrathecal injections in rats as we described previously (36). Chitosan is a biodegradable cationic polysaccharide that binds tightly with the negatively charged siRNA to form the chitosan-siRNA nanoparticles. After recovery from catheter cannulation for 2 days, siRNA (5 µg/20 µl) was intrathecally injected daily for 3 consecutive days. One day after the last chitosan-siRNA injection, we removed the dorsal spinal cords and DRGs at the L5-L6 level.

*Data Analysis*—The HVACC current data were analyzed by using the PulseFit software program (HEKA Instruments). The amplitude of monosynaptic EPSCs was analyzed by using Clampfit 9.2 (Molecular Devices). The whole-cell current volt-age (*I-V*) curves for individual neurons were constructed by calculating the peak inward current at each testing potential and normalizing to the cell capacitance. Conductance voltage (*G-V*) curves were fit with the Boltzmann equation as follows: $G/G_{max} = 1/(1 + \exp(V_{0.5} - V_m/k))$, where $V_{0.5}$ is the voltage for 50% activation or inactivation of HVACCs, and $k$ is a voltage-dependent slope factor. Results were expressed as mean ± S.E. Student's *t* test was used to compare two groups, and one-way analysis of variance (with Tukey's or Dunnett's *post hoc* test) was used to compare multiple groups. $p < 0.05$ was considered statistically significant.

## RESULTS

*High Expression Levels of Cavβ$_3$ and Cavβ$_4$ Subunits in the DRG and Spinal Cord*—To determine which Cavβ subunits are present in the DRG and dorsal spinal cord, we first used reverse transcriptase-PCR and agarose gel electrophoresis to detect the presence of Cavβ$_1$-Cavβ$_4$ mRNA in these tissues. We detected the specific PCR products for Cavβ$_2$ (461 bp), Cavβ$_3$ (301 bp), and Cavβ$_4$ (362 bp) subunits in DRG and spinal cord tissues (Fig. 1*A*), but Cavβ$_1$ mRNA was not detected in the DRG or spinal cord on the agarose gel. However, Cavβ$_1$ (463 bp) was clearly present in G1A1 cells, a HEK293-derived cell line that stably expresses Ca$_v$2.2, Cavβ$_1$, and α$_2$δ subunits (37).

We then quantified the mRNA level of individual Cavβ subunits in the DRG and dorsal spinal cord by using real time PCR. In the L5/L6 DRGs obtained from control rats, the *Ct* values of Cavβ$_1$, Cavβ$_2$, Cavβ$_3$, and Cavβ$_4$ subunits were 28.32, 24.92, 21.74, and 21.59, respectively. Thus, Cavβ$_3$ and Cavβ$_4$ were the most abundant Cavβ subtypes present in the DRG. We calcu-

lated the relative mRNA levels of Cav$\beta$ subunits by using the $2^{-\Delta\Delta Ct}$ method (the *Ct* value of GAPDH was 22.59 in the DRG). When we considered the mRNA level of Cav$\beta_4$ to be 100%, the relative mRNA levels of Cav$\beta_1$, Cav$\beta_2$, and Cav$\beta_3$ subtypes were 0.94, 9.94, and 90.13%, respectively, of Cav$\beta_4$ in the DRG tissue.

In the dorsal spinal cord obtained from control rats, the *Ct* values of the Cav$\beta_1$, Cav$\beta_2$, Cav$\beta_3$, and Cav$\beta_4$ were 29.88, 23.53, 23.18, and 21.19, respectively. The *Ct* value of GAPDH in the spinal cord was 22.61. When we considered the mRNA level of Cav$\beta_4$ to be 100%, the relative mRNA levels of Cav$\beta_1$, Cav$\beta_2$, and Cav$\beta_3$ subtypes were 0.48, 19.75, and 25.17%, respectively, of Cav$\beta_4$ in the spinal cord tissue. Because the expression level of Cav$\beta_1$ in the DRG and spinal cord is very low, we did not study the effect of nerve injury on Cav$\beta_1$ subunit expression in the following experiments.

*Nerve Injury Increases the Expression Level of the Cav$\beta_3$, but Not Cav$\beta_4$, Subunit in the DRG and Spinal Cord*—We next used quantitative PCR to determine how nerve injury changes the expression levels of Cav$\beta_2$, Cav$\beta_3$, and Cav$\beta_4$ subunits in the DRG and dorsal spinal cords contralateral and ipsilateral to SNL. All of the rats developed tactile allodynia and hyperalgesia within 7 days after SNL surgery. We analyzed changes in the mRNA and protein levels of Cav$\beta$ subunits in the DRG and dorsal spinal cord 9 days after SNL. The Cav$\beta_2$ mRNA level in the DRG ipsilateral to SNL was significantly reduced (23.13% of control level). In contrast, the mRNA level of the Cav$\beta_3$ subunit was about 1.57 times greater in the DRG ipsilateral to SNL than in the contralateral DRG. The Cav$\beta_4$ mRNA level in the DRG did not differ significantly between the ipsilateral and contralateral sides (Fig. 1*B*). In the dorsal spinal cord, the Cav$\beta_2$ mRNA level was 53.64% lower in the ipsilateral side than the contralateral side of SNL rats. The mRNA level of Cav$\beta_3$ and Cav$\beta_4$ in the dorsal spinal cord did not differ significantly between the ipsilateral and the contralateral sides (Fig. 1*C*).

Similarly, the Cav$\beta_3$ protein level in the DRG ipsilateral to SNL was about 1.9 times of that in the contralateral side (Fig. 2*A*). However, the Cav$\beta_4$ protein level in the DRG did not differ significantly between the ipsilateral and contralateral sides (Fig. 2*B*). In the dorsal spinal cord, the protein level of Cav$\beta_3$ and Cav$\beta_4$ did not differ significantly between the ipsilateral and contralateral sides of SNL rats (Fig. 2, *A* and *B*). Because the Cav$\beta_2$ protein band of Cav$\beta_1$ and Cav$\beta_2$ in the DRG and dorsal spinal cord was below the detection level in the immunoblots, we did not quantify nerve injury-induced changes in the protein level of these two subunits. Therefore, our findings indicate that peripheral nerve injury primarily increases the expression level of the Cav$\beta_3$ subunit in the DRG.

*Changes in Distribution of the Cav$\beta_3$ Subunit in DRG Neurons after Nerve Injury*—We then used double immunofluorescence labeling and confocal microscopy to examine changes in the distribution of the Cav$\beta_3$ subunit in NF200- and peripherin-immunoreactive DRG neurons in SNL rats. The Cav$\beta_3$ immunoreactivity was present in most DRG neurons immunoreactive to NF200 in control rats (511/547, 93.42%). However, only 44.82% (389/868) peripherin-immunoreactive DRG neurons are co-localized with the Cav$\beta_3$ subunit in sham control rats (Fig. 3). In DRG sections from nerve-injured rats, Cav$\beta_3$
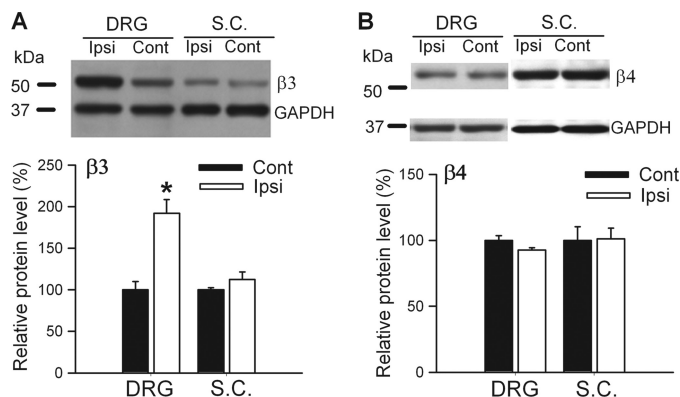


FIGURE 2. **Effect of nerve injury on the protein level of Cav$\beta_3$ and Cav$\beta_4$ subunits in the DRG and dorsal spinal cord tissues.** *A*, Western blots (*top*) and quantification (*bottom*) of the protein amount of Cav$\beta_3$ and Cav$\beta_4$ subunits in the DRG ipsilateral and contralateral to SNL (*n* = 4 in each group). *B*, Western blots (*top*) and quantification (*bottom*) of the protein amount of Cav$\beta_3$ and Cav$\beta_4$ subunits in the dorsal spinal cord (*SC*) ipsilateral and contralateral to SNL (*n* = 4 in each group). *Ipsi*, ipsilateral (nerve injury) side; *Cont*, contralateral (control) side. *, $p < 0.05$, compared with the corresponding value on the contralateral (control) side.

immunoreactivity was present in 95.31% (447/469) NF200-immunoreactive neurons. Notably, the number of peripherin-immunoreactive DRG neurons co-localized with Cav$\beta_3$ (783/822, 95.26%) was significantly increased in nerve-injured rats compared with that in control rats (Fisher's exact test, Fig. 3).

*Nerve Injury Increases HVACC Activity in Small DRG Neurons and Glutamatergic Input to Spinal Dorsal Horn Neurons*— Although complete nerve transection (axotomy) can reduce HVACC activity in DRG neurons (38), the effect of spinal nerve ligation injury on HVACC activity has not been specifically examined. To determine the changes in the HVACC activity in DRG neurons by SNL, we recorded and compared HVACC currents ($I_{Ba}$) in rat DRG neurons 9–10 days after SNL and sham surgery. Neurons were voltage-clamped at −90 mV and depolarized to 0 mV for 200 ms at 1-s intervals. In small (< 30 $\mu$m) DRG neurons, the peak amplitude of $I_{Ba}$ was 1.6 times greater in SNL rats than in sham control rats (Fig. 4*A*). However, in medium (30–40 $\mu$m) and large (> 40 $\mu$m) DRG neurons, there were no significant differences in the current density of $I_{Ba}$ between SNL and sham rats (Fig. 4*A*).

We also determined whether SNL increases glutamatergic input from primary afferent terminals to spinal dorsal horn neurons. EPSCs of lamina II neurons were evoked by electrical stimulation of the dorsal root. The EPSCs were considered monosynaptic if the latency was constant after electrical stimulation (0.2 Hz) and if no conduction failure or increased latency occurred when stimulation frequency was increased to 20 Hz (30, 32). The amplitude of monosynaptic EPSCs of lamina II neurons was significantly increased in the ipsilateral side compared with the contralateral side in SNL rats (Fig. 4*B*). Blocking glutamate AMPA receptors with 20 $\mu$M 6-cyano-7-nitroquinoxaline-2,3-dione abolished EPSCs in all lamina II neurons tested (39).

Next, we determined whether SNL affects activation and inactivation kinetics of $I_{Ba}$ in DRG neurons. The whole-cell HVACC currents in DRG neurons were evoked by a series of depolarizing pulses (from −70 to 50 mV for 150 ms in 10-mV increments) from the holding potential of −90 mV. The cur-
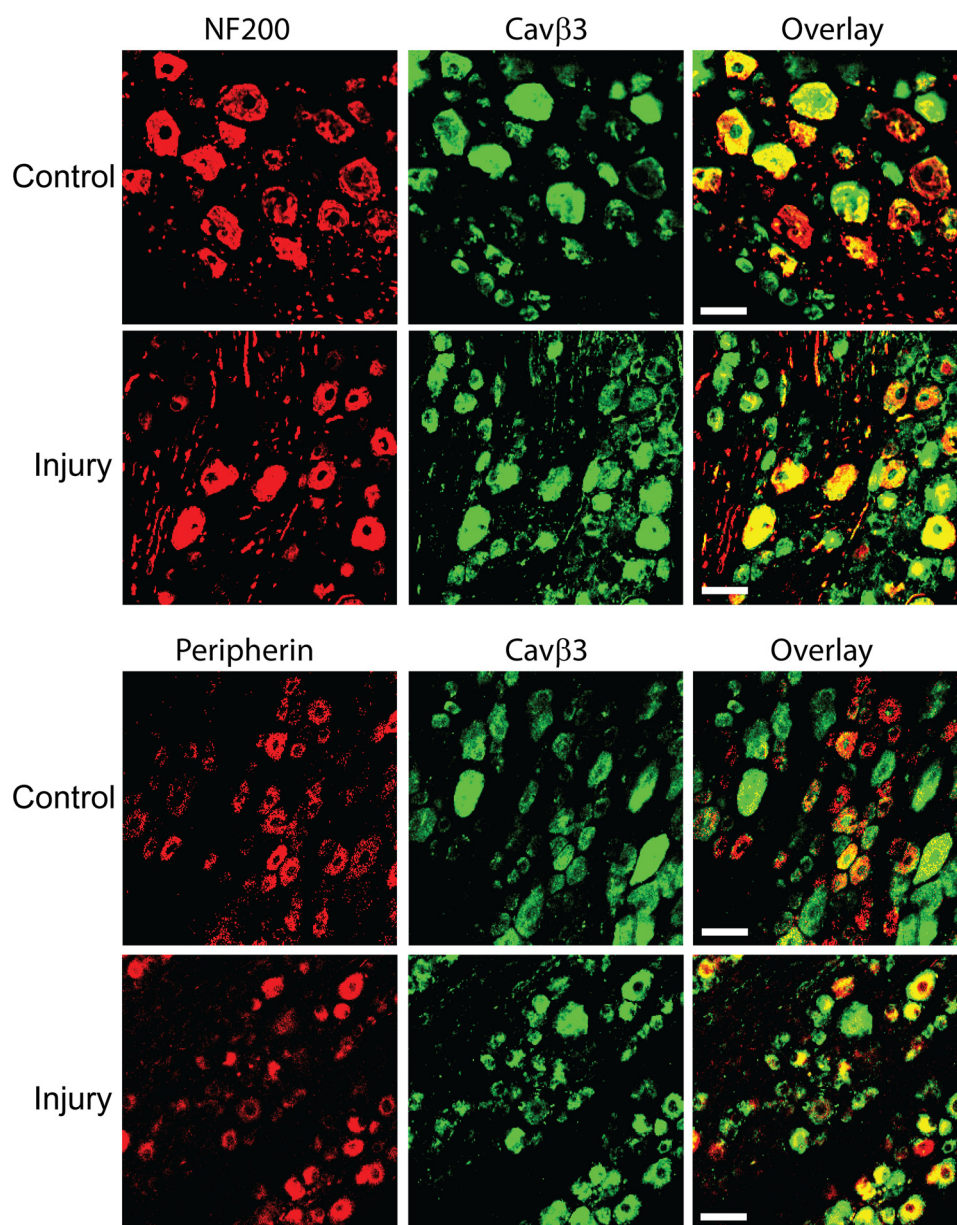
FIGURE 3. **Nerve injury induces increased Cav$\beta_3$ in peripherin-immunoreactive DRG neurons.** Representative confocal images show the distribution of Cav$\beta_3$ immunoreactivity (*green*) in small and large DRG neurons obtained from a sham control and an SNL rat. Neurons that are immunoreactive to NF200 or peripherin are indicated in *red*. *Scale bar,* 50 $\mu$m. All images are single confocal optical sections.

rent density of $I_{Ba}$ in small DRG neurons was largely increased in SNL rats compared with that in sham control rats (Fig. 4C). Although SNL did not alter the current-voltage relationship of $I_{Ba}$, it caused a significant hyperpolarizing shift in $V_{0.5}$ in small DRG neurons (SNL, $-17.5 \pm 0.1$ mV; control, $-13.7 \pm 0.1$ mV) (Fig. 4D). However, SNL did not significantly alter the voltage-dependent inactivation of $I_{Ba}$ in DRG neurons ($n = 15-26$ in each group, see Fig. 4E).

*Down-regulation of Cav$\beta_3$ Subunit Reduces HVACC Activity in DRG Neurons and Glutamatergic Input to Spinal Dorsal Horn Neurons*—Small interfering RNA (siRNA) (20–30 nucleotides) can silence target genes by degrading mRNA with the matching sequence *in vivo* and *in vitro*. It has been shown that 27 nucleotides are more effective in suppressing a target gene than are 21 nucleotides (40). We thus designed two sequences

of siRNA with 27 nucleotides targeting the Cav$\beta_3$ subunit. To ensure the efficient delivery of siRNA into the spinal cord and DRG neurons, we incorporated the siRNA into chitosan (36). In our preliminary experiments, intrathecal treatment with the first Cav$\beta_3$-siRNA (5'-AUGUCUCUUCCUCAUGCUACAU-UGCCU-3') reduced the Cav$\beta_3$ protein level in the DRG by ~50%. However, the second Cav$\beta_3$-siRNA (5'-AUCCACCA-GUCAUUGCUGUACUUCUCU-3') decreased the Cav$\beta_3$ protein level by only 20%. Because the first Cav$\beta_3$ siRNA had a much better effect than did the second Cav$\beta_3$ siRNA, we used the first Cav$\beta_3$-specific siRNA in the following experiments. We injected siRNA (5 $\mu$g) via intrathecal catheters starting on day 10 after SNL for 3 consecutive days.

In the DRG tissues, intrathecal treatment with the Cav$\beta_3$-specific siRNA caused an 82.44% reduction in the Cav$\beta_3$ mRNA
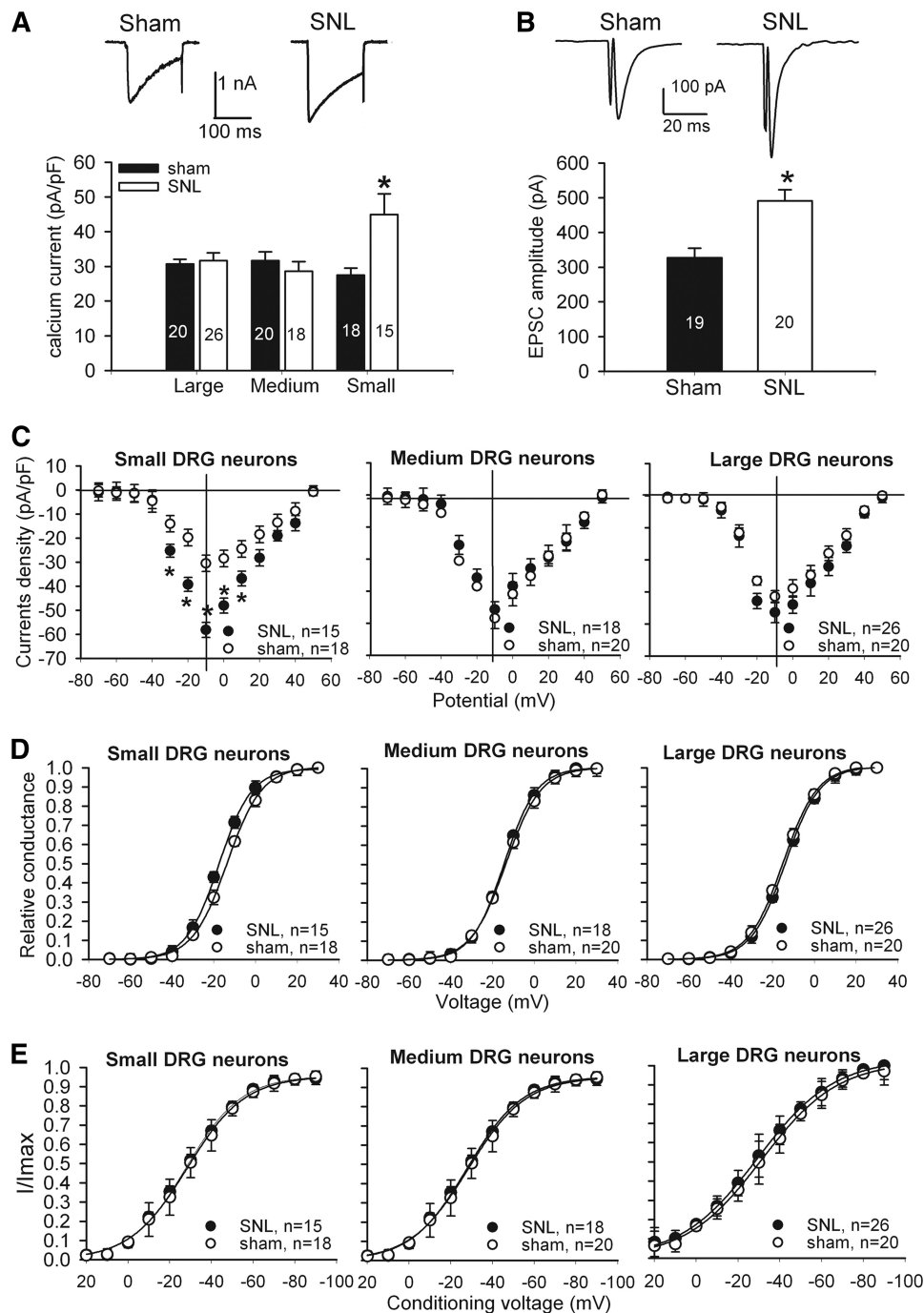
FIGURE 4. **Effects of nerve injury on HVACC activity of DRG neurons and monosynaptic EPSCs of spinal dorsal horn neurons.** *A,* original current traces (*upper panel*) show HVACC currents in small DRG neurons from a control and a nerve-injured rat. Group data (*lower panel*) show that SNL increased HVACC currents in small, but not large and medium, DRG neurons. Neurons were voltage-clamped at $-90$ mV and depolarized to 0 mV for 200 ms. The number of cells in each group is indicated in the *column. B,* representative traces and group data show the monosynaptic EPSCs of lamina II neurons in spinal cords obtained from sham control ($n = 19$) and SNL ($n = 20$) rats. *C,* effect of SNL on the current-voltage relationship of HVACCs in small, medium, and large DRG neurons. *D,* effect of SNL on voltage-dependent activation of HVACCs in small, medium, and large DRG neurons. Note that SNL shifted voltage-dependent activation of HVACCs to the left only in small DRG neurons. The $V_{0.5}$ in control and SNL rats was $-13.7 \pm 0.1$ and $-17.5 \pm 0.1$ mV ($p < 0.05$), respectively. The slope factor in control and SNL rats was $8.33 \pm 0.2$ and $7.80 \pm 0.1$ mV ($p > 0.05$), respectively. *E,* effect of SNL on voltage-dependent inactivation of HVACCs in small, medium, and large DRG neurons. *, $p < 0.05$, compared with the corresponding value in the sham group. *pF,* picofarad.

level in the ipsilateral side and a 41.75% reduction in the contralateral side of SNL rats, compared with that in control siRNA-treated rats (Fig. 5*A*). In the dorsal spinal cord, intrathecal treatment with Cavβ3-specific siRNA decreased the Cavβ3 mRNA level by 40% in both sides, compared with that in control siRNA-treated rats (Fig. 5*B*). To ensure the specificity of the Cavβ3

siRNA, we also determined the effect of Cavβ3-specific siRNA on the Cavβ4 mRNA level in the DRG and dorsal spinal cord. The Cavβ3 siRNA had no significant effects on the Cavβ4 mRNA level in the DRG and spinal cord of SNL rats (Fig. 5, *A* and *B*)

Treatment with the Cavβ3-specific siRNA caused a larger reduction in the Cavβ3 protein level in the DRG on the ipsilat-
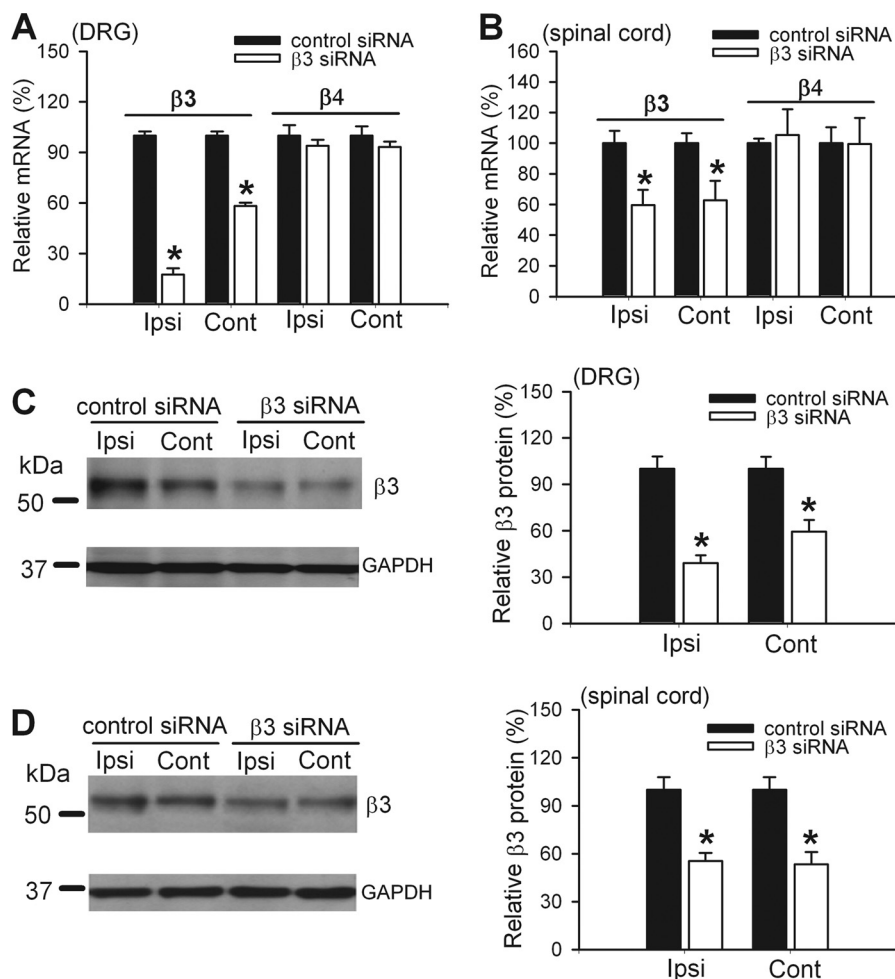
FIGURE 5. **Effect of intrathecal treatment with Cav$\beta_3$-specific siRNA (5 $\mu$g per day for 3 days) on the expression level of Cav$\beta_3$ in the DRG and spinal cord of SNL rats.** *A*, effect of Cav$\beta_3$-specific siRNA on the mRNA level of Cav$\beta_3$ and Cav$\beta_4$ in the DRG of SNL rats ($n = 4$ in each group). *B*, effect of Cav$\beta_3$-specific siRNA on the mRNA level of Cav$\beta_3$ and Cav$\beta_4$ in the dorsal spinal cord of SNL rats ($n = 4$ in each group). *C*, Western blots (*left*) and quantification (right, $n = 4$ in each group) of the protein amount of the Cav$\beta_3$ subunit in the DRG ipsilateral and contralateral to SNL in rats treated with Cav$\beta_3$-specific siRNA or control siRNA. *D*, Western blots (*left*) and quantification (*right*, $n = 4$ in each group) of the protein amount of the Cav$\beta_3$ subunit in the dorsal spinal cord ipsilateral and contralateral to SNL in rats treated with Cav$\beta_3$-specific siRNA or control siRNA. *Ipsi*, ipsilateral (nerve injury) side; *Cont*, contralateral (control) side. *, $p < 0.05$, compared with the corresponding value in control siRNA-treated group.

eral side (60.90% decrease) than on the contralateral side (40.92% decrease) (Fig. 5C). Also, the amount of the Cav$\beta_3$ protein on both sides of the dorsal spinal cord was significantly reduced (by ~40%) in rats treated with the Cav$\beta_3$-specific siRNA, compared with that in control siRNA-treated rats (Fig. 5D).

To determine the contribution of the Cav$\beta_3$ subunit to increased HVACC activity in DRG neurons of SNL rats, we examined the effect of Cav$\beta_3$-specific siRNA on the current density of $I_{Ba}$ in DRG neurons. Intrathecal treatment with Cav$\beta_3$-siRNA caused a large decrease in the amplitude of $I_{Ba}$ in small DRG neurons ipsilateral to SNL, compared with the control siRNA-treated rats (Fig. 6, *A* and *C*). By comparison, treatment with Cav$\beta_3$-siRNA caused a smaller reduction in the current density of $I_{Ba}$ in small DRG neurons on the contralateral side, compared with the control siRNA-treated rats. Also, treatment with Cav$\beta_3$-siRNA caused a depolarizing shift of $V_{0.5}$ in small DRG neurons ipsilateral to SNL (control siRNA, $-14.37 \pm 0.1$; Cav$\beta_3$-specific siRNA, $-11.02 \pm 0.1$ mV; see Fig. 6D).

Intrathecal treatment with Cav$\beta_3$-specific siRNA also significantly decreased the amplitude of monosynaptic EPSCs of spinal lamina II neurons evoked from the dorsal root in SNL rats (Fig. 6B). This Cav$\beta_3$ siRNA effect was much more prominent in the ipsilateral than in the contralateral side of the spinal cord in SNL rats. Collectively, these data indicate that up-regulation of the Cav$\beta_3$ subunit in primary afferent neurons contributes to increased activity of HVACCs and glutamatergic input from primary afferents to spinal dorsal horn neurons caused by nerve injury.

*Down-regulation of Cav$\beta_3$ Subunit at the Spinal Level Reduces Neuropathic Pain*—In addition, we performed nociceptive behavioral tests to determine whether up-regulation of the Cav$\beta_3$ subunit in DRG neurons contributes to pain hypersensitivity induced by nerve injury. SNL significantly reduced the pressure and tactile withdrawal thresholds of the hind paw on the ipsilateral side compared with the contralateral side (Fig. 7). Intrathecal treatment with Cav$\beta_3$-specific siRNA (5 $\mu$g/day for 3 days) or control siRNA had no significant effect on the ambulation behavior of rats. Compared with the control siRNA
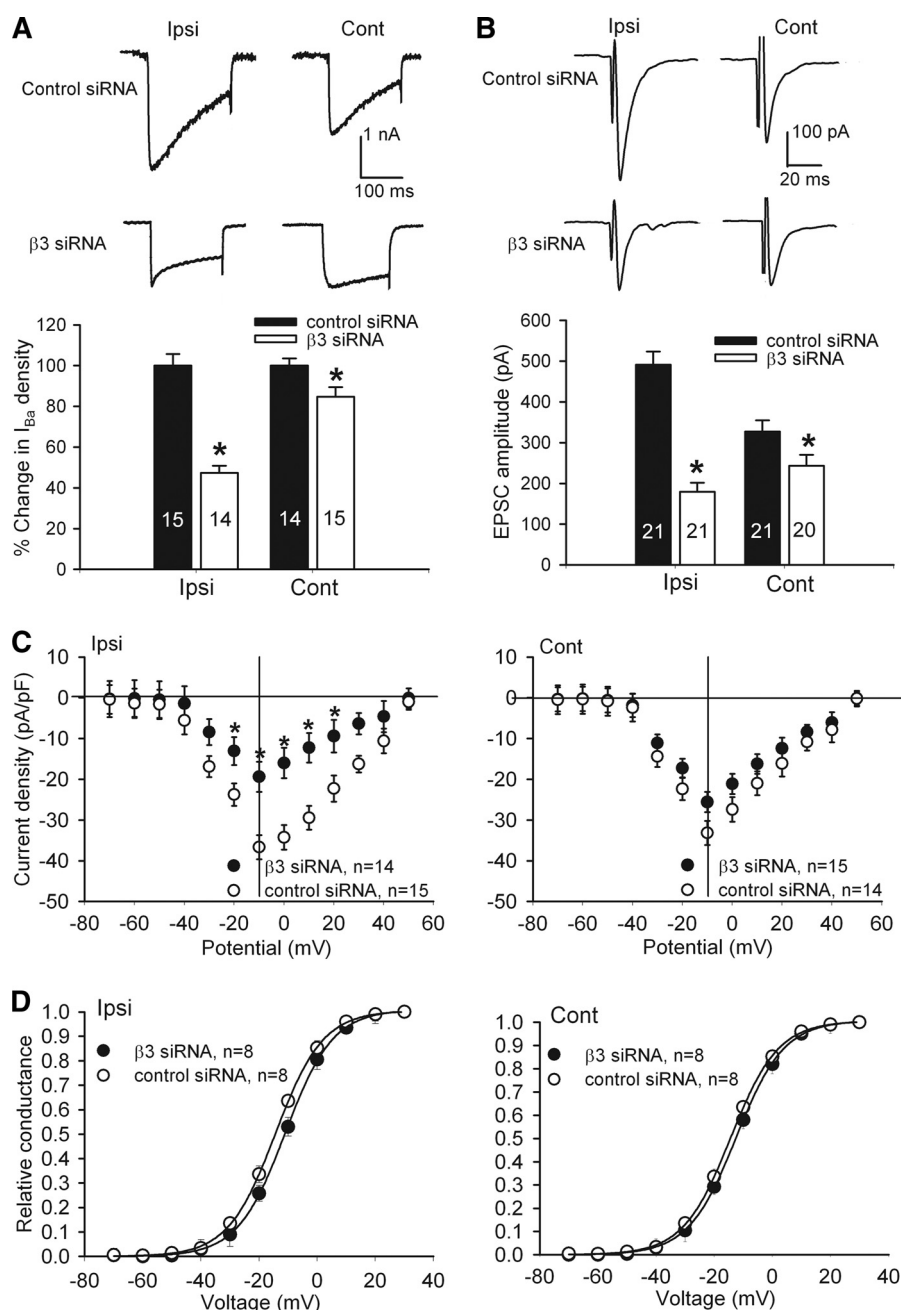
FIGURE 6. **Effects of intrathecal treatment with Cav$\beta_3$-specific siRNA on HVACC activity in DRG neurons and monosynaptic EPSCs of spinal dorsal horn neurons of SNL rats.** *A,* original traces and group data show the effect of Cav$\beta_3$-specific siRNA on HVACC current in small DRG neurons ipsilateral and contralateral to SNL. The number of cells in each group is indicated in the *column. B,* representative traces and summary data show the effect of Cav$\beta_3$-specific siRNA on the amplitude of monosynaptic EPSCs of lamina II neurons in the spinal cord of SNL rats. *C,* effect of Cav$\beta_3$-specific siRNA on the current-voltage relationship of HVACCs in small DRG neurons ipsilateral and contralateral to SNL. *D,* effect of Cav$\beta_3$-specific siRNA on voltage-dependent activation of HVACCs in small DRG neurons ipsilateral and contralateral to SNL. Note that treatment with Cav$\beta_3$-specific siRNA shifted the voltage-dependent activation of HVACCs to the right in small DRG neurons ipsilateral to SNL. The $V_{0.5}$ in control-siRNA and Cav$\beta_3$-specific siRNA groups was $-14.37 \pm 0.1$ and $-11.02 \pm 0.1$ mV ($p <$ 0.05), respectively. The slope factor in control-siRNA and Cav$\beta_3$-specific siRNA groups was $8.20 \pm 0.1$ and $8.20 \pm 0.2$ mV ($p > 0.05$), respectively. *Ipsi,* ipsilateral (nerve injury) side; *Cont,* contralateral (control) side. *, $p < 0.05$, compared with the corresponding value in control siRNA-treated group.

treatment, intrathecal administration of Cav$\beta_3$-specific siRNA gradually reversed the pressure and tactile withdrawal thresholds of the hind paw ipsilateral to SNL (Fig. 7). The pressure withdrawal threshold and tactile withdrawal threshold of the hind paw ipsilateral to SNL were completely normalized 3 days after treatment with Cav$\beta_3$-specific siRNA. However, treatment with control siRNA did not significantly alter the pressure and tactile withdrawal thresholds of the hind paw ipsilateral to

SNL. Also, the Cav$\beta_3$-specific siRNA had no significant effect on the pressure and tactile withdrawal thresholds of the hind paw contralateral to SNL (Fig. 7).

## DISCUSSION

In this study, we determined how nerve injury affects the expression of Cav$\beta$ subunits in primary sensory neurons and whether such changes contribute to increased HVACC cur-
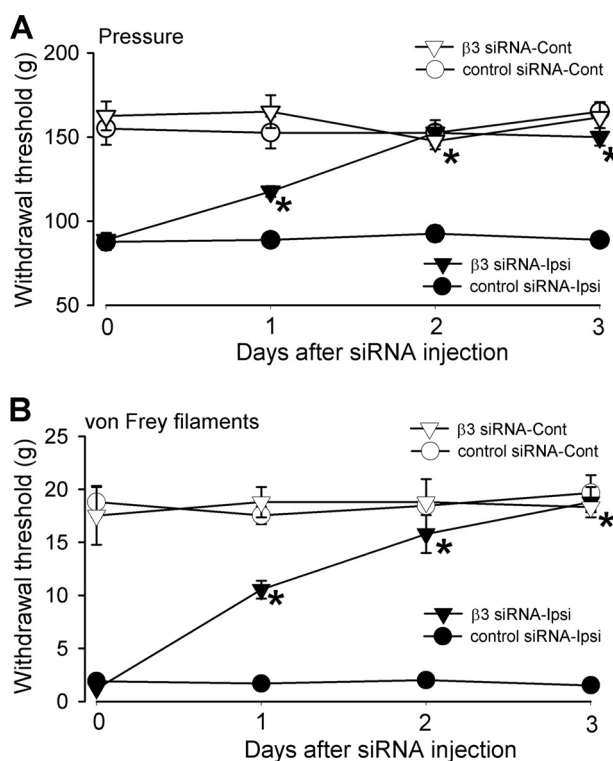
FIGURE 7. **Effects of intrathecal treatment with Cav$\beta_3$-specific siRNA (5 $\mu$g per day for 3 days) on nociceptive and tactile withdrawal thresholds of hind paws in SNL rats.** *A,* time course effects of control siRNA and Cav$\beta_3$-specific siRNA on the nociceptive withdrawal threshold, tested with a noxious pressure stimulus, of hind paws ipsilateral and contralateral to SNL ($n = 6$ rats in each group). *B,* time course effects of control siRNA and Cav$\beta_3$-specific siRNA on the tactile withdrawal threshold, measured with von Frey filaments, of hind paws ipsilateral and contralateral to SNL ($n = 6$ rats in each group). Note that Cav$\beta_3$-specific siRNA, but not control siRNA, increased nociceptive and tactile withdrawal thresholds of hind paws ipsilateral to SNL. *Ipsi,* ipsilateral (nerve injury) side; *Cont,* contralateral (control) side. *, $p < 0.05$, compared with the base-line value in Cav$\beta_3$-specific siRNA-treated group.

rents and pain hypersensitivity induced by nerve injury. Persistent increases in nociceptive input from injured peripheral nerves are an important feature of chronic neuropathic pain (3, 22, 23). We found that SNL significantly increased the current density of HVACCs in small DRG neurons. SNL also shifted the voltage-dependent activation of HVACCs in the hyperpolarizing direction, suggesting that HVACCs open more readily in these DRG neurons in the neuropathic pain condition. We found that SNL also significantly increased the amplitude of monosynaptic EPSCs of dorsal horn neurons evoked from the dorsal root. Our data suggest that glutamatergic input from primary afferents to spinal dorsal horn neurons is potentiated in neuropathic pain. Blocking N-type HVACCs at the spinal level is highly effective in the treatment of severe pain in patients (41, 42), and knock-out of N-type HVACCs in mice reduces neuropathic pain symptoms (43). Also, reducing the expression of Ca$_v$1.2 (one of the L-type HVACCs) attenuates neuropathic pain in SNL rats (44). Although L- and N-type HVACCs are involved in the generation of abnormal ectopic discharges of DRG neurons caused by nerve injury (45), the molecular mechanisms underlying increased HVACC activity in DRG neurons and nociceptive input in neuropathic pain are not fully known.

The pore-forming $\alpha_1$ subunit is often associated with two core auxiliary subunits consisting of the membrane-anchored, largely extracellular $\alpha_2\delta$ subunit and the cytoplasmic Cav$\beta$ subunit (5). The $\alpha_1$ subunits are the primary determinants of both channel biophysics and pharmacology, whereas Cav$\beta$, $\alpha_2\delta$, and $\gamma$ subunits are regarded as regulators of HVACC functions. There are four subfamilies of Cav$\beta$ subunits that are mainly expressed in the excitable tissues such as the brain, heart, and muscles. Cav$\beta_1$ is mainly expressed in the hippocampus and skeletal muscle (46), whereas Cav$\beta_2$ is mostly expressed in the heart (47, 48). Cav$\beta_3$ is expressed not only in several brain regions but also in the heart and lungs (47, 49). Cav$\beta_4$ is strongly expressed in the cerebellum (14). It has been reported that the mRNA level of several $\alpha_1$ subunits in DRG tissues is reduced by sciatic nerve injury (50). Although nerve injury can increase $\alpha_2\delta$ expression in DRG neurons (51, 52), it is uncertain whether this change is casually related to increased HVACC activity in DRG neurons by nerve injury. $\alpha_1$B (N-type) is the predominant $\alpha_1$ subtype that mediates HVACC currents in DRG neurons (25). The $\beta_3$ subunit regulates both L- and N-type HVACCs (53, 54). By using quantitative PCR and Western blot analyses, we found that Cav$\beta_3$ and Cav$\beta_4$ are the most predominant Cav$\beta$ subtypes distributed in the DRG and dorsal spinal cord tissues. Furthermore, we found that SNL caused a significant increase in the mRNA and protein levels of the Cav$\beta_3$, but not Cav$\beta_4$, subunit in the DRG, suggesting that the Cav$\beta_3$ expression level is increased in primary afferent neurons in neuropathic pain. Our immunolabeling results provide further evidence that increased Cav$\beta_3$ expression occurs predominantly in peripherin-positive small-sized DRG neurons after nerve injury. We noted that nerve injury significantly decreased the mRNA level of Cav$\beta_2$ in the DRG and spinal cord. Because the basal expression level of Cav$\beta_2$ in the DRG and spinal cord was extremely low, the reduced Cav$\beta_2$ expression level may have little impact on HVACC activity in primary sensory neurons. Alternatively, the reduced Cav$\beta_2$ level may free up HVACC $\alpha_1$ subunits and allow them to form more $\alpha_1$-Cav$\beta_3$ complexes in injured DRG neurons.

Although the important role of the Cav$\beta_3$ subunit in the regulation of HVACCs has been shown in cell lines (12, 26), their contribution to increased HVACC activity in neuropathic pain has not been demonstrated in native neurons due to the lack of specific pharmacological approaches. In this study, we demonstrated that intrathecal treatment with Cav$\beta_3$-specific siRNA conjugated to chitosan selectively and efficiently knocked down the expression level of the Cav$\beta_3$ subunit in the DRG and dorsal spinal cord. Importantly, down-regulation of Cav$\beta_3$ by siRNA caused a large reduction in the current density of HVACCs and a depolarizing shift in the voltage-dependent activation of HVACCs in small DRG neurons ipsilateral to SNL. By comparison, Cav$\beta_3$-specific siRNA had little effect on HVACC currents in small DRG neurons on the control side of SNL rats. Cav$\beta_3$-specific siRNA also reduced voltage-dependent activation and inactivation of HVACC currents in small DRG neurons, which is consistent with the role of Cav$\beta_3$ in the control of HVACC gating (15). Thus, our results indicate that up-regulation of the $\beta_3$ subunit plays a key role in increased HVACC activity in injured DRG neurons in neuropathic pain. Because treatment with Cav$\beta_3$-specific siRNA attenuated the amplitude

of monosynaptic EPSCs of dorsal horn neurons more on the ipsilateral side than on the contralateral side of SNL rats, this finding provides further evidence that up-regulation of the $Cav\beta_3$ subunit contributes to increased HVACC activity and neurotransmitter release from the primary afferent terminals in the spinal dorsal horn in neuropathic pain. An increase in the $Cav\beta_3$ subunit could increase the $\alpha_1$-$Cav\beta_3$ binding and augment HVACC activity by promoting $\alpha_1$ subunit expression on the plasma membrane after nerve injury.

Another salient finding of our study is that down-regulation of the $Cav\beta_3$ subunit at the spinal level by chitosan-siRNA profoundly reduced mechanical hyperalgesia and tactile allodynia induced by SNL in rats. We found that intrathecal treatment with $Cav\beta_3$-specific siRNA for 3 days completely normalized pain hypersensitivity in SNL rats. Interestingly, although knockdown of $Cav\beta_3$ also decreased the expression level of $Cav\beta_3$ in DRG neurons and spinal cord contralateral to SNL, intrathecal treatment with $Cav\beta_3$-specific siRNA had no significant effect on the nociceptive and tactile thresholds of the hind paw contralateral to SNL. This finding suggests that down-regulation of $Cav\beta_3$ at the spinal level alone does not impair normal nociception. Consistent with our finding with the siRNA approach, it has been reported that knock-out of $Cav\beta_3$ in mice reduces acute inflammatory pain but has little effect on normal nociceptive thresholds in response to noxious heat and mechanical stimuli (55). The profound effect of $Cav\beta_3$-specific siRNA on SNL-induced pain hypersensitivity suggests that the increased $Cav\beta_3$ expression level in DRG neurons becomes critically important for augmented HVACC activity and nociceptive input in neuropathic pain. This notion is supported by our finding that the $Cav\beta_3$-siRNA effect on the HVACC currents of small DRG neurons was much more pronounced on the ipsilateral (injury) side than the contralateral (control side) of SNL rats. Furthermore, the inhibitory effect of $Cav\beta_3$-specific siRNA on the evoked EPSC amplitude of spinal dorsal horn neurons was much greater on the ipsilateral side than on the contralateral side of SNL rats. Another possibility is that nerve injury may increase the uptake of chitosan-siRNA by injured primary afferent neurons. This is because $Cav\beta_3$-specific siRNA treatment produced a greater effect on the $Cav\beta_3$ expression level in the DRG on the ipsilateral side than on the contralateral side of SNL rats.

In summary, we demonstrated in this study that the $Cav\beta_3$ subunit is up-regulated and critically contributes to increased HVACC activity in DRG neurons and nociceptive input to spinal dorsal horn neurons in neuropathic pain. Down-regulation of the $Cav\beta_3$ subunit at the spinal level normalizes neuropathic pain but has no significant effect on normal nociception. Directly blocking N-type HVACCs at the spinal level often produces intolerable adverse effects (42, 56) and thus has limited clinical use in the treatment of chronic pain. Our findings suggest the $Cav\beta_3$ subunit may represent a new target for neuropathic pain treatment with a reduced adverse effect profile. Many aminopyridine analogs can modulate HVACC activity through the $Cav\beta$ subunit (26). These compounds could be modified to inhibit $Cav\beta_3$ subunit function to reduce increased HVACC activity and nociceptive input in neuropathic pain. Therefore, our study provides important information about the molecular mechanisms underlying increased HVACC activity in primary sensory neurons by nerve injury. This new information improves our understanding of neuroplastic changes associated with neuropathic pain and helps the design of novel analgesics for neuropathic pain treatment.

## REFERENCES

1. Dworkin, R. H., O'Connor, A. B., Backonja, M., Farrar, J. T., Finnerup, N. B., Jensen, T. S., Kalso, E. A., Loeser, J. D., Miaskowski, C., Nurmikko, T. J., Portenoy, R. K., Rice, A. S., Stacey, B. R., Treede, R. D., Turk, D. C., and Wallace, M. S. (2007) Pharmacologic management of neuropathic pain. Evidence-based recommendations. *Pain* **132,** 237–251

2. Campero, M., Serra, J., Marchettini, P., and Ochoa, J. L. (1998) Ectopic impulse generation and autoexcitation in single myelinated afferent fibers in patients with peripheral neuropathy and positive sensory symptoms. *Muscle Nerve* **21,** 1661–1667

3. Gracely, R. H., Lynch, S. A., and Bennett, G. J. (1992) Painful neuropathy. Altered central processing maintained dynamically by peripheral input. *Pain* **51,** 175–194

4. Catterall, W. A., and Few, A. P. (2008) Calcium channel regulation and presynaptic plasticity. *Neuron* **59,** 882–901

5. Catterall, W. A. (2000) Structure and regulation of voltage-gated $Ca^{2+}$ channels. *Annu. Rev. Cell Dev. Biol.* **16,** 521–555

6. Kang, M. G., Chen, C. C., Felix, R., Letts, V. A., Frankel, W. N., Mori, Y., and Campbell, K. P. (2001) Biochemical and biophysical evidence for $\gamma 2$ subunit association with neuronal voltage-activated $Ca^{2+}$ channels. *J. Biol. Chem.* **276,** 32917–32924

7. Catterall, W. A., Perez-Reyes, E., Snutch, T. P., and Striessnig, J. (2005) International Union of Pharmacology. XLVIII. Nomenclature and structure-function relationships of voltage-gated calcium channels. *Pharmacol. Rev.* **57,** 411–425

8. Andrade, A., Sandoval, A., González-Ramírez, R., Lipscombe, D., Campbell, K. P., and Felix, R. (2009) The $\alpha_2\delta$ subunit augments functional expression and modifies the pharmacology of Ca(V)1.3 L-type channels. *Cell Calcium* **46,** 282–292

9. Luo, Z. D., Chaplan, S. R., Higuera, E. S., Sorkin, L. S., Stauderman, K. A., Williams, M. E., and Yaksh, T. L. (2001) Up-regulation of dorsal root ganglion $\alpha_2\delta$ calcium channel subunit and its correlation with allodynia in spinal nerve-injured rats. *J. Neurosci.* **21,** 1868–1875

10. De Waard, M., Pragnell, M., and Campbell, K. P. (1994) $Ca^{2+}$ channel regulation by a conserved $\beta$ subunit domain. *Neuron* **13,** 495–503

11. Pragnell, M., De Waard, M., Mori, Y., Tanabe, T., Snutch, T. P., and Campbell, K. P. (1994) Calcium channel $\beta$-subunit binds to a conserved motif in the I-II cytoplasmic linker of the $\alpha$1-subunit. *Nature* **368,** 67–70

12. Yamaguchi, H., Hara, M., Strobeck, M., Fukasawa, K., Schwartz, A., and Varadi, G. (1998) Multiple modulation pathways of calcium channel activity by a $\beta$ subunit. Direct evidence of $\beta$ subunit participation in membrane trafficking of the $\alpha$1C subunit. *J. Biol. Chem.* **273,** 19348–19356

13. Hofmann, F., Biel, M., and Flockerzi, V. (1994) Molecular basis for $Ca^{2+}$ channel diversity. *Annu. Rev. Neurosci.* **17,** 399–418

14. Ludwig, A., Flockerzi, V., and Hofmann, F. (1997) Regional expression and cellular localization of the $\alpha$1 and $\beta$ subunit of high voltage-activated calcium channels in rat brain. *J. Neurosci.* **17,** 1339–1349

15. Buraei, Z., and Yang, J. (2010) The $\beta$ subunit of voltage-gated $Ca^{2+}$ channels. *Physiol. Rev.* **90,** 1461–1506

16. Gregg, R. G., Messing, A., Strube, C., Beurg, M., Moss, R., Behan, M., Sukhareva, M., Haynes, S., Powell, J. A., Coronado, R., and Powers, P. A. (1996) Absence of the $\beta$ subunit (cchb1) of the skeletal muscle dihydropyridine receptor alters expression of the $\alpha$1 subunit and eliminates excitation-contraction coupling. *Proc. Natl. Acad. Sci. U.S.A.* **93,** 13961–13966

17. Weissgerber, P., Held, B., Bloch, W., Kaestner, L., Chien, K. R., Fleischmann, B. K., Lipp, P., Flockerzi, V., and Freichel, M. (2006) Reduced cardiac L-type $Ca^{2+}$ current in $Ca_V\beta_2^{-/-}$ embryos impairs cardiac development and contraction with secondary defects in vascular maturation. *Circ. Res.* **99,** 749–757

18. Murakami, M., Nakagawasai, O., Yanai, K., Nunoki, K., Tan-No, K., Ta-

dano, T., and Iijima, T. (2007) Modified behavioral characteristics following ablation of the voltage-dependent calcium channel β3 subunit. *Brain Res.* **1160,** 102–112

19. Burgess, D. L., Jones, J. M., Meisler, M. H., and Noebels, J. L. (1997) Mutation of the Ca$^{2+}$ channel β subunit gene *Cchb4* is associated with ataxia and seizures in the lethargic (lh) mouse. *Cell* **88,** 385–392

20. Kim, S. H., and Chung, J. M. (1992) An experimental model for peripheral neuropathy produced by segmental spinal nerve ligation in the rat. *Pain* **50,** 355–363

21. Chen, S. R., Eisenach, J. C., McCaslin, P. P., and Pan, H. L. (2000) Synergistic effect between intrathecal non-NMDA antagonist and gabapentin on allodynia induced by spinal nerve ligation in rats. *Anesthesiology* **92,** 500–506

22. Chen, S. R., Cai, Y. Q., and Pan, H. L. (2009) Plasticity and emerging role of BKCa channels in nociceptive control in neuropathic pain. *J. Neurochem.* **110,** 352–362

23. Zhou, H. Y., Chen, S. R., Chen, H., and Pan, H. L. (2011) Functional plasticity of group II metabotropic glutamate receptors in regulating spinal excitatory and inhibitory synaptic input in neuropathic pain. *J. Pharmacol. Exp. Ther.* **336,** 254–264

24. Chaplan, S. R., Bach, F. W., Pogrel, J. W., Chung, J. M., and Yaksh, T. L. (1994) Quantitative assessment of tactile allodynia in the rat paw. *J. Neurosci. Methods* **53,** 55–63

25. Wu, Z. Z., and Pan, H. L. (2004) High voltage-activated Ca$^{2+}$ channel currents in isolectin B(4)-positive and -negative small dorsal root ganglion neurons of rats. *Neurosci. Lett.* **368,** 96–101

26. Wu, Z. Z., Li, D. P., Chen, S. R., and Pan, H. L. (2009) Aminopyridines potentiate synaptic and neuromuscular transmission by targeting the voltage-activated calcium channel β subunit. *J. Biol. Chem.* **284,** 36453–36461

27. Pan, H. L., Khan, G. M., Alloway, K. D., and Chen, S. R. (2003) Resiniferatoxin induces paradoxical changes in thermal and mechanical sensitivities in rats. Mechanism of action. *J. Neurosci.* **23,** 2911–2919

28. Cervero, F., and Iggo, A. (1980) The substantia gelatinosa of the spinal cord. A critical review. *Brain* **103,** 717–772

29. Chen, S. R., Chen, H., Yuan, W. X., and Pan, H. L. (2011) Increased presynaptic and postsynaptic α$_2$-adrenoceptor activity in the spinal dorsal horn in painful diabetic neuropathy. *J. Pharmacol. Exp. Ther.* **337,** 285–292

30. Zhou, H. Y., Chen, S. R., Chen, H., and Pan, H. L. (2010) Opioid-induced long term potentiation in the spinal cord is a presynaptic event. *J. Neurosci.* **30,** 4460–4466

31. Zhou, H. Y., Zhang, H. M., Chen, S. R., and Pan, H. L. (2008) Increased C-fiber nociceptive input potentiates inhibitory glycinergic transmission in the spinal dorsal horn. *J. Pharmacol. Exp. Ther.* **324,** 1000–1010

32. Wang, X. L., Zhang, H. M., Li, D. P., Chen, S. R., and Pan, H. L. (2006) Dynamic regulation of glycinergic input to spinal dorsal horn neurons by muscarinic receptor subtypes in rats. *J. Physiol.* **571,** 403–413

33. Frey, U. H., Bachmann, H. S., Peters, J., and Siffert, W. (2008) PCR amplification of GC-rich regions. "Slowdown PCR." *Nat. Protoc.* **3,** 1312–1317

34. Chen, C. C., England, S., Akopian, A. N., and Wood, J. N. (1998) A sensory neuron-specific, proton-gated ion channel. *Proc. Natl. Acad. Sci. U.S.A.* **95,** 10240–10245

35. Perry, M. J., Lawson, S. N., and Robertson, J. (1991) Neurofilament immunoreactivity in populations of rat primary afferent neurons. A quantitative study of phosphorylated and nonphosphorylated subunits. *J. Neurocytol.* **20,** 746–758

36. Cai, Y. Q., Chen, S. R., Han, H. D., Sood, A. K., Lopez-Berestein, G., and Pan, H. L. (2009) Role of M2, M3, and M4 muscarinic receptor subtypes in the spinal cholinergic control of nociception revealed using siRNA in rats. *J. Neurochem.* **111,** 1000–1010

37. McDavid, S., and Currie, K. P. (2006) G-proteins modulate cumulative inactivation of N-type (Ca$_v$2.2) calcium channels. *J. Neurosci.* **26,** 13373–13383

38. Abdulla, F. A., and Smith, P. A. (2001) Axotomy- and autotomy-induced changes in Ca$^{2+}$ and K$^+$ channel currents of rat dorsal root ganglion neurons. *J. Neurophysiol.* **85,** 644–658

39. Pan, Y. Z., and Pan, H. L. (2004) Primary afferent stimulation differentially potentiates excitatory and inhibitory inputs to spinal lamina II outer and inner neurons. *J. Neurophysiol.* **91,** 2413–2421

40. Kim, D. H., Behlke, M. A., Rose, S. D., Chang, M. S., Choi, S., and Rossi, J. J. (2005) Synthetic dsRNA Dicer substrates enhance RNAi potency and efficacy. *Nat. Biotechnol.* **23,** 222–226

41. Staats, P. S., Yearwood, T., Charapata, S. G., Presley, R. W., Wallace, M. S., Byas-Smith, M., Fisher, R., Bryce, D. A., Mangieri, E. A., Luther, R. R., Mayo, M., McGuire, D., and Ellis, D. (2004) Intrathecal ziconotide in the treatment of refractory pain in patients with cancer or AIDS. A randomized controlled trial. *JAMA* **291,** 63–70

42. Schmidtko, A., Lötsch, J., Freynhagen, R., and Geisslinger, G. (2010) Ziconotide for treatment of severe chronic pain. *Lancet* **375,** 1569–1577

43. Saegusa, H., Kurihara, T., Zong, S., Kazuno, A., Matsuda, Y., Nonaka, T., Han, W., Toriyama, H., and Tanabe, T. (2001) Suppression of inflammatory and neuropathic pain symptoms in mice lacking the N-type Ca$^{2+}$ channel. *EMBO J.* **20,** 2349–2356

44. Fossat, P., Dobremez, E., Bouali-Benazzouz, R., Favereaux, A., Bertrand, S. S., Kilk, K., Léger, C., Cazalets, J. R., Langel, U., Landry, M., and Nagy, F. (2010) Knockdown of L calcium channel subtypes. Differential effects in neuropathic pain. *J. Neurosci.* **30,** 1073–1085

45. Liu, X., Zhou, J. L., Chung, K., and Chung, J. M. (2001) Ion channels associated with the ectopic discharges generated after segmental spinal nerve injury in the rat. *Brain Res.* **900,** 119–127

46. Powers, P. A., Liu, S., Hogan, K., and Gregg, R. G. (1992) Skeletal muscle and brain isoforms of a β-subunit of human voltage-dependent calcium channels are encoded by a single gene. *J. Biol. Chem.* **267,** 22967–22972

47. Hullin, R., Singer-Lahat, D., Freichel, M., Biel, M., Dascal, N., Hofmann, F., and Flockerzi, V. (1992) Calcium channel β subunit heterogeneity. Functional expression of cloned cDNA from heart, aorta, and brain. *EMBO J.* **11,** 885–890

48. Chu, P. J., Larsen, J. K., Chen, C. C., and Best, P. M. (2004) Distribution and relative expression levels of calcium channel β subunits within the chambers of the rat heart. *J. Mol. Cell. Cardiol.* **36,** 423–434

49. Castellano, A., Wei, X., Birnbaumer, L., and Perez-Reyes, E. (1993) Cloning and expression of a third calcium channel β subunit. *J. Biol. Chem.* **268,** 3450–3455

50. Kim, D. S., Yoon, C. H., Lee, S. J., Park, S. Y., Yoo, H. J., and Cho, H. J. (2001) Changes in voltage-gated calcium channel α(1) gene expression in rat dorsal root ganglia following peripheral nerve injury. *Brain Res. Mol. Brain Res.* **96,** 151–156

51. Luo, Z. D., Calcutt, N. A., Higuera, E. S., Valder, C. R., Song, Y. H., Svensson, C. I., and Myers, R. R. (2002) Injury type-specific calcium channel α2δ-1 subunit up-regulation in rat neuropathic pain models correlates with antiallodynic effects of gabapentin. *J. Pharmacol. Exp. Ther.* **303,** 1199–1205

52. Newton, R. A., Bingham, S., Case, P. C., Sanger, G. J., and Lawson, S. N. (2001) Dorsal root ganglion neurons show increased expression of the calcium channel α2δ-1 subunit following partial sciatic nerve injury. *Brain Res. Mol. Brain Res.* **95,** 1–8

53. Murakami, M., Yamamura, H., Suzuki, T., Kang, M. G., Ohya, S., Murakami, A., Miyoshi, I., Sasano, H., Muraki, K., Hano, T., Kasai, N., Nakayama, S., Campbell, K. P., Flockerzi, V., Imaizumi, Y., Yanagisawa, T., and Iijima, T. (2003) Modified cardiovascular L-type channels in mice lacking the voltage-dependent Ca$^{2+}$ channel β3 subunit. *J. Biol. Chem.* **278,** 43261–43267

54. Namkung, Y., Smith, S. M., Lee, S. B., Skrypnyk, N. V., Kim, H. L., Chin, H., Scheller, R. H., Tsien, R. W., and Shin, H. S. (1998) Targeted disruption of the Ca$^{2+}$ channel β3 subunit reduces N- and L-type Ca$^{2+}$ channel activity and alters the voltage-dependent activation of P/Q-type Ca$^{2+}$ channels in neurons. *Proc. Natl. Acad. Sci. U.S.A.* **95,** 12010–12015

55. Murakami, M., Fleischmann, B., De Felipe, C., Freichel, M., Trost, C., Ludwig, A., Wissenbach, U., Schwegler, H., Hofmann, F., Hescheler, J., Flockerzi, V., and Cavalié, A. (2002) Pain perception in mice lacking the β3 subunit of voltage-activated calcium channels. *J. Biol. Chem.* **277,** 40342–40351

56. Wallace, M. S., Rauck, R., Fisher, R., Charapata, S. G., Ellis, D., and Dissanayake, S. (2008) Intrathecal ziconotide for severe chronic pain. Safety and tolerability results of an open-label, long term trial. *Anesth. Analg.* **106,** 628–637